RESEARCH ARTICLE

Editorial Process: Submission:02/20/2025 Acceptance:08/14/2025 Published:08/23/2025

Biosynthesis of Copper Nanoparticles Using *Passiflora* Flower Extract and Study their Antimicrobial, Antioxidant and Anticancer Activity

Ons Hussain Sahib[1], Lubna Z Mohammed[2], Montadher Ali Mahdi[3]*

Abstract

Objective: Copper nanoparticles (CuNPs) have received interest due to their antibacterial, antioxidant, and anticancer effects. However, current synthesis methods frequently use harmful substances. Green synthesis with plant extracts provides a safer, more environmentally friendly option. This study looks at the production of CuNPs with *Passiflora* flower extract and assesses their biological activity. **Methods:** *Passiflora* extract was used as a reducing and stabilizing agent in the synthesis of CuNPs. UV-Vis spectroscopy, FTIR, SEM, XRD, and AFM were used to characterize the samples. The biological activities were evaluated using DPPH antioxidant assays, antimicrobial tests against bacterial and fungal strains, and MTT assays on MCF7 cancer cells and HFF normal cells. **Results:** The CuNPs produced had a spherical form with an average size of 10-20 nm. Antioxidant activity was high, with an IC_{50} of 98.94 µg/ml. CuNPs showed broad-spectrum antibacterial activity, especially against *Staphylococcus aureus* and *Candida albicans*. The cytotoxicity assay revealed preferential toxicity against MCF7 breast cancer cells (IC_{50} = 47.01 µg/ml) while preserving normal HFF cells (IC_{50} = 128.35 µg/ml). These findings are consistent with prior research, confirming the potential biomedical applications of CuNPs. **Conclusion:** Green-synthesized CuNPs have substantial antioxidant, antibacterial, and anticancer properties. Their specific toxicity to cancer cells demonstrates their potential as a Nano medicine option. Further research into *in vivo* efficacy and long-term safety is recommended.

Keywords: Copper nanoparticles- *Passiflora* flower extract- antioxidant- antimicrobial- anticancer

Asian Pac J Cancer Prev, **26 (8)**, 2953-2963

Introduction

Nanotechnology has evolved as a transformative field with applications in medical, electronics, and environmental science [1]. Among the various nanomaterials synthesized, copper nanoparticles (CuNPs) have received great interest due to their unique physicochemical features include high conductivity, catalytic activity, and strong antibacterial activities [2]. Despite their benefits, traditional nanoparticle production processes can use dangerous chemicals and require a lot of energy, causing environmental and health issue [3].

The green synthesis of nanoparticles tackles these issues by using plant extracts, bacteria, and other biological components as reducing and stabilizing agents [4]. This environmentally benign strategy not only reduces the usage of harmful chemicals, but it also improves the biocompatibility of the synthesized nanoparticles, hence broadening their potential biological applications. Plants, in particular, are great candidates for green synthesis due to their abundant supply of secondary metabolites that include flavonoids, tannins, alkaloids, and phenolic chemicals, which aid in nanoparticle formation [5]. *Passiflora*, sometimes known as passion flower, is a medicinal plant noted for its antioxidant, anti-inflammatory, and anticancer qualities [6]. Its bioactive components make it an excellent choice for green nanoparticle manufacturing. In this study, we investigated the ability of *Passiflora* extract to produce copper nanoparticles in an environmentally friendly manner [7]. The CuNPs were thoroughly characterized to determine their structural, morphological, and chemical properties.

Breast cancer is among the most common cancers affecting women worldwide [8]. It is caused by the uncontrolled proliferation of cells in breast tissue and can spread to other parts of the body if not diagnosed and treated promptly. Breast cancer is generally treated with a mix of surgery, radiation therapy, chemotherapy, and targeted therapies [9]. However, the emergence of resistance to current treatments emphasizes the need for new therapeutic options. Nanoparticles, particularly copper nanoparticles synthesized using green technologies, have showed promise in increasing cancer therapy efficacy by triggering apoptosis, suppressing proliferation, and

[1]*College of Science, Mustansiriyah university, Baghdad, Iraq.* [2]*College of Science for women, University of Baghdad, Baghdad, Iraq.* [3]*National Center for Cancer Research, University of Baghdad, Baghdad, Iraq. *For Correspondence: montadhermalky@yahoo.com*

reducing adverse effects [10].

Furthermore, the nanoparticles' biological activities, such as antibacterial, antioxidant, and anticancer impacts, were assessed to determine their usefulness in the biomedical sector. This study intends to add to the expanding body of knowledge on green nanotechnology by emphasizing the importance of plant-mediated nanoparticle production as a sustainable alternative to traditional approaches.

Materials and Methods

Plant Material Collection and Preparation

Passiflora flowers leaves were harvested from healthy plants in the early morning to preserve their phytochemicals. The leaves were cleaned with distilled water to eliminate contaminants before being dried in a shady, ventilated space for two weeks with a fine mesh covering to prevent contamination. After drying, the leaves were crushed into a fine powder and stored in airtight containers to preserve their bioactive qualities [11]. A botanist from Al-Mustansiriyah University's Department of Biology, College of Science recognized and authenticated the plant species.

Extraction Process for Passiflora flower leaves

Depending on the method used by Sunitha et al. [12]. a total of 40 grams of dried and crushed *Passiflora* leaves were extracted with 200 ml of distilled water. The extraction has been carried out using a Soxhlet apparatus with continuous reflux for 2 hours at 60°C. This method enabled a successful extraction of bioactive chemicals found in plant material. After extraction, the solution was taken from the heat and allowed to cool gradually to room temperature. The extract was then left undisturbed for 24 hours to allow any suspended particles to settle and to gather as many bioactive chemicals as possible. On the following day, the extract was filtered using fine-grade filter paper to separate the liquid phase from residual plant debris, yielding a pure, concentrated *Passiflora* extract free from impurities. This filtrate was subsequently stored in sterile, airtight containers at low temperatures to prevent degradation and preserve the integrity of the bioactive constituents.

Qualitative analysis for phytochemical components in Passiflora flower leaves

The phytochemical testing of *Passiflora* flower leaves was a typical approach for analyzing the metabolites in the floral extract. The extract was evaluated for proteins, saponins, alkaloids, carbohydrates, phenolic compounds, steroids, triterpenoids, tannins, flavonoids, and Vitamin C using established processes and methodologies by Mahdi et al. [13].

Fourier-Transform Infrared Spectroscopy (FTIR) for Passiflora flower leaves

FTIR analysis was used to detect the functional groups in the *Passiflora* extract. The plant material subsequently dried, crushed to a fine powder, and solvent extracted using ethanol. The extract had been concentrated by evaporating the solvent beneath reduced pressure with a rotary evaporator. A little amount of the dried extract was applied directly on the FTIR spectrometer's attenuated total reflectance (ATR) crystal without further preparation. Spectral data from 4000 to 400 cm^{-1} were acquired and analyzed to identify important bioactive components in the extract [14].

Gas Chromatography-Mass Spectrometry (GC-MS) for Passiflora flower leaves

By using the method of Paulraj et al. [15] with a slight modification. 2 mL sample of *Passiflora* extracted was centrifuged at 4,000 rpm over 10 minutes to remove solid leftovers and the resulting supernatant was filtered through Whatman No.1 filter paper. Liquid-liquid extraction was repeated twice with 10 mL of ethyl acetate at a 2:1 ratio. The ethyl acetate fractions were mixed and concentrated under decreased pressure at 55°C using a rotary evaporator. The injection temperature proved 250°C in split less mode, with a one-minute sampling period. The system ran at 100 kPa, with a column flow of 1.2 mL/min and a 15:1 split ratio. The mass spectrometry was carried out at an ion source temperature of 200°C and an interface temperature of 250°C. The scan range was m/z 40-700, and data collection began at 3.50 minutes and terminated 27 minutes. The spectra were analyzed using the NIST library to identify compounds by matching them to known references, yielding precise molecular information on the extract's constituents.

Biosynthesis of copper nanoparticles (CuNPs) using Passiflora flower leaves

Copper nanoparticles were produced by dissolving copper nitrate in distilled water to produce a 0.1 M solution. A volume of 100 mL of copper nitrate solution was combined with 100 mL of *Passiflora* botanical extract in an alkaline medium with a pH of 9 at 20 degrees . Experimenting with different concentrations, volumes, temperatures, and pH values revealed the ideal synthesis conditions. The generated nanoparticles were analyzed with UV-Vis spectroscopy to determine the circumstances that produced the maximum nanoparticle concentration. Based on these findings, the standard processing parameters were determined. The solution was allowed to react for 24 hours, and the color gradually changed from clear yellow to dark greenish brown, suggesting the creation of copper nanoparticles. Following the reaction, the nanoparticles were isolated by centrifugation at an appropriate speed to separate the precipitate [16]. The precipitate was washed three times with distilled water to ensure the removal of impurities and unreacted materials. The collected precipitate was left to dry at room temperature for three days and subsequently stored for further analysis and applications (Figure 1).

Characterization of Copper Nanoparticles
UV-Vis spectroscopy

The UV-Vis spectral study was performed using a spectrophotometer from PG Instruments Limited in T80, Germany. The decrease of CuNPs was confirmed by UV-vis spectroscopy at constant intervals ranging from

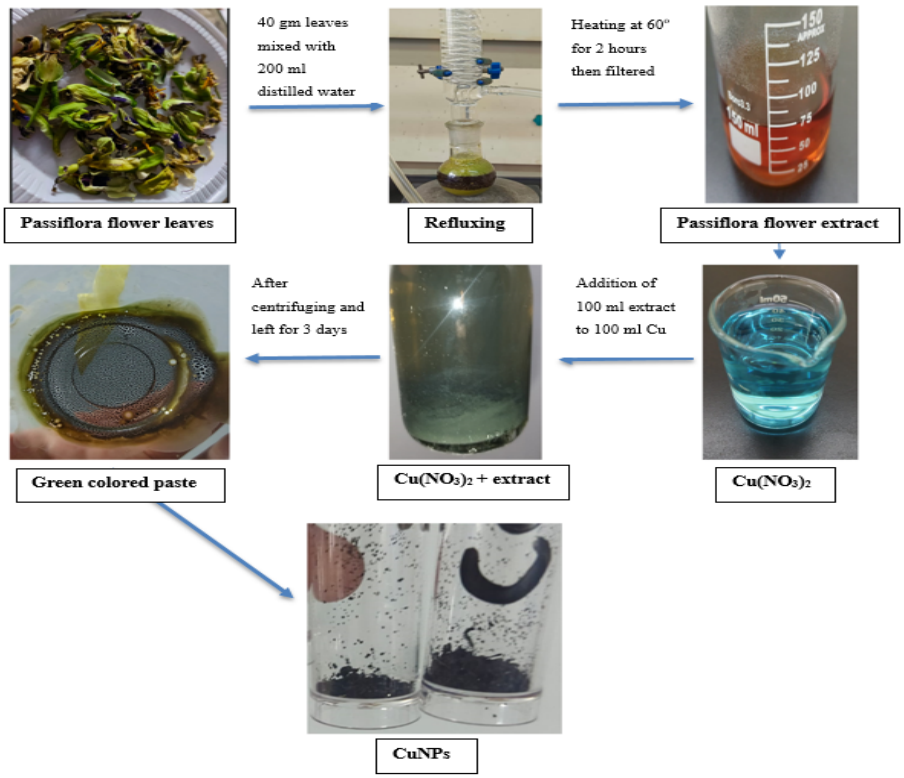

Figure 1. Mechanism and Steps to Synthesize CuNPs.

400 to 1,000 nm. After pipetting 3 ml of the substance into a test tube, it is tested at room temperature. The blank is made of deionized water. The absorbance of the CuNPs solution during surface Plasmon resonance should range from 400 to 500 nm [17].

Atomic Force Microscopy (AFM)

An atomic force microscope (AFM) (Model AA3000, Angstrom Advance Inc., USA) is used to determine the sizes and dispersion of metal nanoparticles. AFM samples in liquid suspension are prepared using the dropper evaporation technique. Pour a droplet of liquid onto a cover slide approximately 2 by 2 cm. Either leave the sample overnight in a dust-free environment or use the heater (set to low) to speed up the drying process before wiping.

Scanning Electron Microscopy (SEM) and Energy Dispersive X-ray (EDX)

SEM is utilized to determine the morphology and shape of biologically synthesized CuNPs (SEM-Angstrom Advanced Inc.-AIS2300C). An INCA EDX probe is used to do energy dispersive X-ray microanalysis.

X-ray Diffraction (XRD)

The University of Kashan used a Bruker d8 Advance X-ray diffracto-meter with CuKα radiation (λ = 1.5406 Å), 40 kV-40mA, and 2θ/θ scanning mode to record the XRD pattern of the Copper nanoparticles. Data is collected with a step of 0.0202 degrees, covering the 2θ range of 30 to 80 degrees. Peak locations are compared to the standard data to determine the crystalline phases [18].

Quantitative determination of Free radical scavenging activity assay (DPPH method)

According to Mahdi et al. [13]. *Passiflora* flower leaf extract, CuNPs, and standard ascorbic acid (Vitamin C) (0.5 mL) were mixed with 1 mL of DPPH solution (2 mL of 0.013g/L DPPH) in methanol. The decrease of DPPH by *Passiflora* flower leaf extract and CuNPs is measured at 517 nm after 30 minutes compared to a blank. The residual radical ratio in reaction medium is calculated by dividing the sample absorbance by that of the DPPH control and multiplying by 100. The amount of sample required to reduce the initial DPPH concentration by 50%, or IC_{50}, was visually computed.

Antibacterial activity for Passiflora flower leaves and CuNPs

The standard agar-well diffusion technique for bactericidal susceptibility was used to assess the presence of antibacterial activity in *Passiflora* flower leaf extract and CuNPs against *Escherichia coli*, *Klebsiellasp*, *Staphylococcus epidermidis*, *Staphylococcus aureus*, and one fungus (*Candida albicans*). The medium was sterilized in an autoclave at 120°C. The medium was then transferred to sterilized Petri plates and maintained at 37°C till solidification. The bacterial strains were distributed on the Petri plates using a loop. A gel pierce was used on each plate to create a single 4mm diameter well. *Passiflora* flower leaf extract and CuNPs (5µl) was put to the wells. The plates were incubated at 37°C for 24 hours. The studies were carried out in triplicate, and the zone of inhibition was measured [19].

Cytotoxicity of AgNPs

The human liver cancer cell line was derived from the division for tissue culture at (ICCMGR). The cells are grown in 75 cm^2 tissue culture containers under controlled conditions of 5% CO_2 and 37°C, with humidity closely monitored. The RPMI-1640 culture media manufactured by Sigma Chemicals in England were used. The tested reagent was diluted with 10% fetal bovine serum (FBS) from ICCMGR and 1% penicillin-streptomycin (100 U/mL penicillin and 100 µg/mL streptomycin) from Lilly in Italy. Along with the experiment [20].

In a 96-well microliter plate. Cancer cells are cultivated and exposed to various concentrations of nano and vincristine. The concentration of cancer cells in each well will steadily increase during the logarithmic evolution phase, and the efficacy of the tested solutions will be assessed after two incubation periods of 24 and 72 hours. Each well holds 7 x 10^3 cells. Cancer cells are cultivated in a growth medium with 10% calf serum. The plates are then placed in an incubator set to 37°C for 24 hours to facilitate cancer cell adhesion. A maintenance medium is used to prepare concentrations of nano and vincristine ranging from 1 to 1,000 µg/mL. The dilutions are done in six fold increments. After 24 hours of incubation, cells are subjected to every tested concentration and duplicated six times with a volume of 200µl each. In the control group, each well received only 200 µl of maintenance medium. The exposure times are 24 and 72 hours. The plates are hermetically sealed with self-adhesive material and returned to the incubator. Next, the cells are stained using MTT dye. The optical density of each well is determined using a micro-ELISA reader with a wavelength of 550 nm. The following calculation is used to quantify the inhibitor rate [21].

Growth inhibtion rate (optical density of control-optical density of the test)/(optical density of control)*100

Statistical Analysis

(SAS) is used to identify the elements that influence cytotoxicity. The means of the individuals are matched using the Least Significant Difference (LSD) and Tukey tests.

Results

Phytochemical Analysis of Passiflora Extract

The quantitative analysis for *Passiflora* extracts shows that it contains lots of phytochemical compounds, the study shows the presence of proteins, carbohydrates, tannins, phenolic compounds, flavonoids, and steroids. While the absence of saponins in the utilized tests. The high level and diversity of the phytochemical compounds in *Passiflora* extracts show the ability to work as a reducing and capping agent. The results of qualitative analysis shown in Table 1.

Fourier-Transform Infrared Spectroscopy (FTIR) for Passiflora flower leaves

The FTIR spectrum of aqueous extract in *Passiflora* shows multiple strfong peaks, indicating the existence of several functional groups. The broad and powerful absorption band at 3,417.86 cm^{-1} corresponds to the stretching vibrations for hydroxyl (-OH) groups, suggesting the presence of phenols and alcohols. The peaks at 2,918.30 cm^{-1} and 2,850.79 cm^{-1} show C-H stretching in alkanes, confirming the existence of saturated hydrocarbons. The signal at 1,735.93 cm^{-1} is attributable to the stretching vibrations for carbonyl (C=O) groups, which are often associated via esters, ketones, or aldehydes. The band at 1,635.64 cm^{-1} shows C=C stretching vibrations, indicating the existence of alkenes or aromatic chemicals. The peak at 1,543.05 cm^{-1} represents N-H bending, indicating amines or amides.

The absorption bands at 1,419.61 cm^{-1} and 1,338.60 cm^{-1} correspond to the bending vibrations for C-H bonds in alkanes or CH_2 scissoring. The signal at 1,247.94 cm^{-1} implies C-O stretching, which might be esters, ethers, or carboxylic acids. Peaks between 1,105.21 cm^{-1} and 1,053.13 cm^{-1} correspond to C-O-C stretching vibrations, indicating the existence of polysaccharides or glyosidic linkages. The peaks at 923.91 cm^{-1} and 833.24 cm^{-1} represent the out-of-plane twisting vibrations of aromatic C-H bonds, confirming the existence of aromatic rings. The absorptions at 761.87 cm^{-1} and 619.16 cm^{-1} indicate the existence of substituted aromatic compounds. The peaks at 536.22 cm^{-1} and 420.48 cm^{-1} may indicate trace quantities of metal complexes or inorganic substances.

Overall, the FTIR examination of *Passiflora*'s aqueous extract reveals an existence of hydroxyl, carbonyl, aromatic, as well as alkane functional groups, indicating a diverse composition of bioactive chemicals including phenolic, flavonoids, and terpenoids. Figure 2 shows the FTIR chart for *Passiflora* extract.

Gas Chromatography-Mass Spectrometry (GC-MS) for Passiflora flower leaves

The GC-MS study of the *Passiflora* extract indicated

Table 1. Phytochemical Screening for Reseda Lutea Aqueous Extract

Components	Reagent	Note	Results
Proteins	Biuret test	Purple blue	Positive
Steroids	Liebermann Burchard	Yellow ppt	Positive
Carbohydrates	Molish test	Violet ring	Positive
Alkoloids	Mayer's reagent	White ppt	Positive
Phenolic compounds	Fwrric chloride test	Green ppt	Positive
(Tannin and Flavonoid))	Lead acetate	Yellow white ppt	Positive
Saponins	Fast stirring	Dense foam for long time	Negative

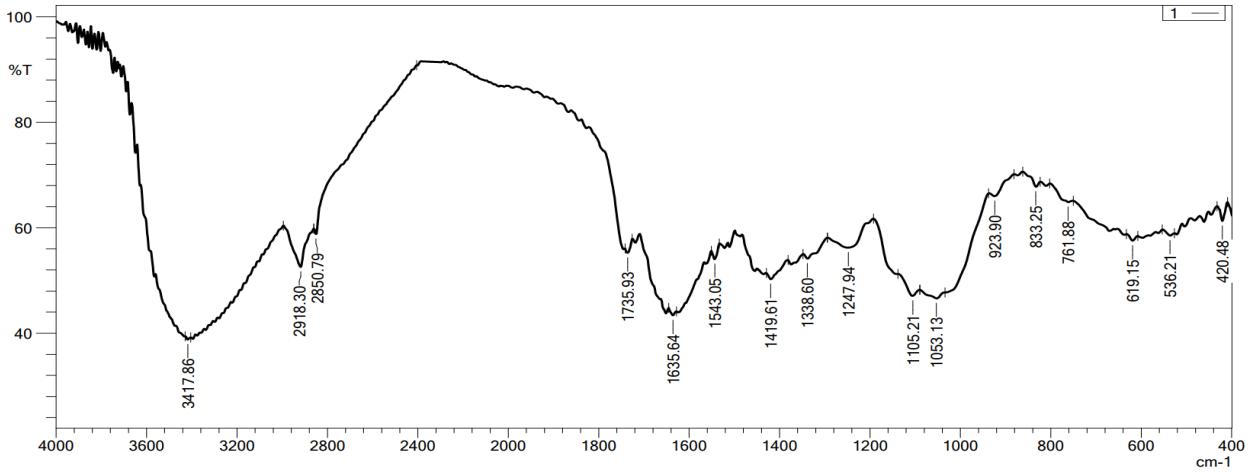

Figure 2. FTIR Analysis for Passiflora Extracts

the presence of 25 bioactive chemicals that have important pharmacological and industrial implications. Among the discovered chemicals, n-Hexadecanoic acid (palmitic acid) was recognized as a prominent ingredient. This saturated fatty acid is known for its antioxidant, antibacterial, and anti-inflammatory characteristics, making it useful in medicinal and cosmetic products. Oleic acid (9-Octadecenoic acid), cis-10-Nonadecenoic acid, 1,14-Dibromotetradecane, and cis-Vaccenic acid are also important chemicals that help to reduce the risk of cardiovascular disease by improving cholesterol levels. Furthermore, cis-10-Nonadecenoic acid and cis-vaccenic acid promote heart health while also preventing bacterial and fungal infections, increasing the extract's efficiency as a natural antibacterial agent. Collectively, these chemicals emphasize *Passiflora* extract's potential therapeutic effects in pharmaceutical and health applications, making it an attractive candidate for the development of anti-inflammatory, antioxidant, and antibacterial products. The results of GC-Mass analysis shown in Figure 3.

Biosynthesis of copper nanoparticles (CuNPs) using Passiflora flower leaves

UV-Vis spectroscopy

The UV-Vis absorption spectrum depicts the optical characteristics of copper nanoparticles produced using

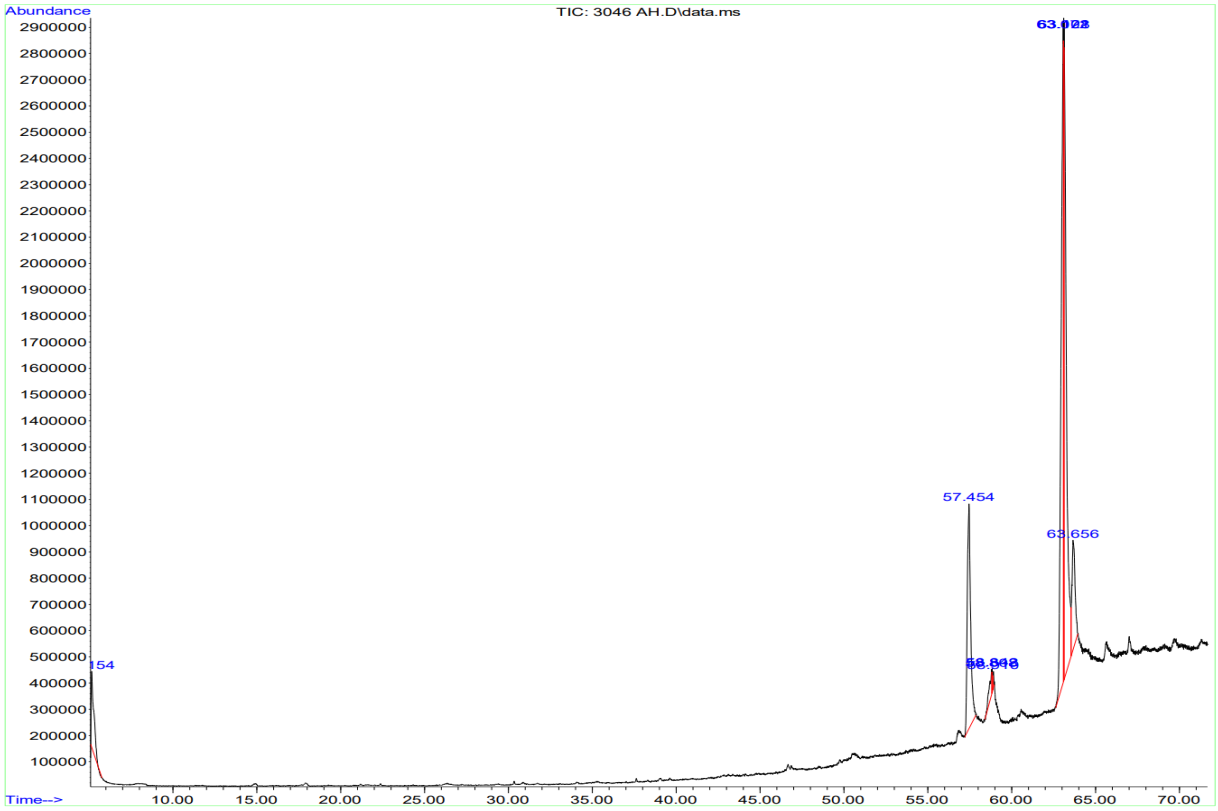

Figure 3. The GC-Mass Analysis for Passiflora Extract

green synthesis. The scan spans a wavelength range of 200 nm to 750 nm. A prominent peak appears at approximately 400 nm, with a maximum absorbance of 1.05, indicating the surface plasmon resonance (SPR) of copper nanoparticles. This peak confirms the successful production of copper nanoparticles. The dramatic increase in absorbance in the 350-400 nm region reflects the excitation of surface electrons, whereas the broad breadth of the peak suggests a polydisperse nanoparticle distribution or variations in particle size. The slow fall in absorbance below 450 nm implies negligible aggregation, implying that the nanoparticles are stable. The position and structure of the SPR peak provide information about particle size and stability, including peaks around 400 nm often indicating copper nanoparticles less than 100 nm. UV-Vis spectroscopy is critical in characterizing nanoparticles, and the distinct SPR peak in the spectrum corresponds to literature findings for copper nanoparticles, demonstrating the success and stability of the synthesis method. Figure 4 shows the UV-Visible spectrum for CuNPs synthesized by *Passiflora* extract.

Atomic Force Microscopy (AFM)

The results of the AFM investigation demonstrate the effective synthesis of CuNPs with suitable properties for nanoscale applications. The average particle diameter of 115.7 nm is well within the nanoscale range, and the majority of particles are tiny to medium in size (less than 200 nm), indicating regulated growth and minimal aggregation. The presence of smaller particles with a minimum diameter of 7.255 nm demonstrates the efficacy of the synthesis process in creating ultra-fine nanoparticles that maximize surface area. The surface coverage of 32.77% and particle density of 14,002,704 particles/mm² show high yield and homogeneous deposition over the substrate, enhancing the functionalization potential for antibacterial, catalysis, and coating applications. The average greatest height (Z-max) of 773.6 nm indicates a degree of vertical growth, which contributes to increased performance while maintaining surface homogeneity. While a few bigger particles (aggregation and agglutination) are present, they make up a small proportion of the distribution and have no meaningful impact on the overall quality of the nanoparticles. These findings demonstrate the efficacy of the synthesis approach in manufacturing high-density, homogeneous copper nanoparticles appropriate for a variety of biological and medical applications. AFM analysis report shown in Figure 5.

Scanning Electron Microscopy (SEM)

The SEM image from copper (Cu) nanoparticles reveals important information about the shape, size distribution, and surface properties of the synthesized material. Direct particle size measurements revealed diameters of around 71.10 nm, 62.95 nm, and 56.41 nm, all falling inside the nanoscale range. The particles had a usually spherical or near-spherical shape, indicating uniform nucleation and regulated development during the green synthesis process with *Passiflora* extract. Surface texture analysis of the smallest particles reveals a smooth appearance, which is useful for applications that need few surface flaws. The clustering of particles in specific places indicates that, while individual nanoparticles appear well-formed, there might be a localized agglomeration. The nanoparticles appear well-dispersed, with low agglomeration, which is crucial for increasing surface area and functional characteristics. The comparatively narrow size distribution indicates the efficacy of the green synthesis process, which uses plant extracts as reducing and stabilizing agents. This environmentally safe technique simplifies the synthesis process while simultaneously lowering the possibility of hazardous consequences. The small particle size increases surface area, which improves nanoparticles' capacity to neutralize free radicals. Copper nanoparticles are recognized for their potent antibacterial properties. The homogeneous size ensures consistent contact with bacterial cells, resulting in effective bacterial suppression. Smaller nanoparticles can infiltrate cells more easily, potentially improving their

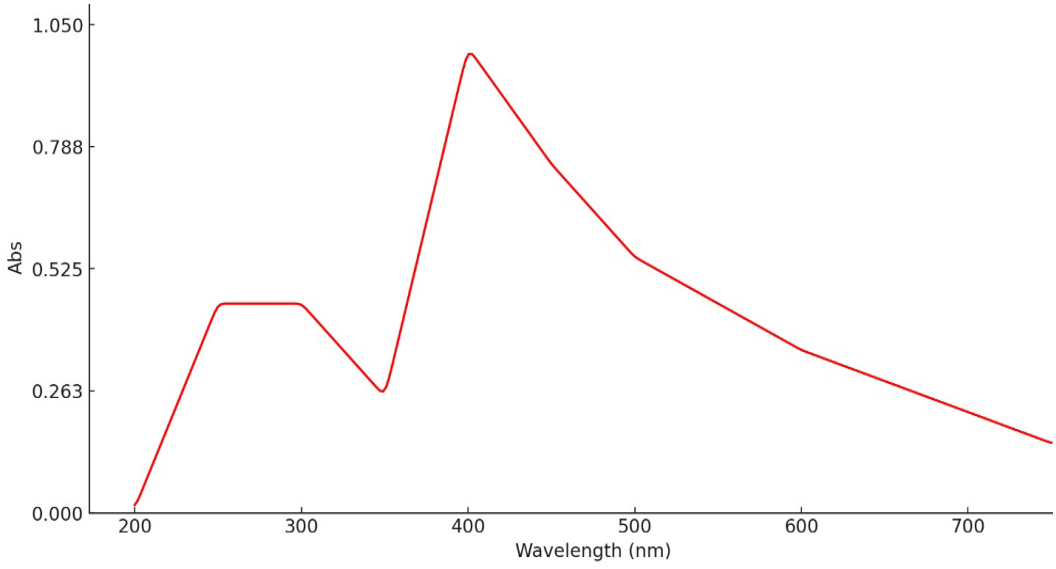

Figure 4. UV-Visible Spectrum for CuNPs

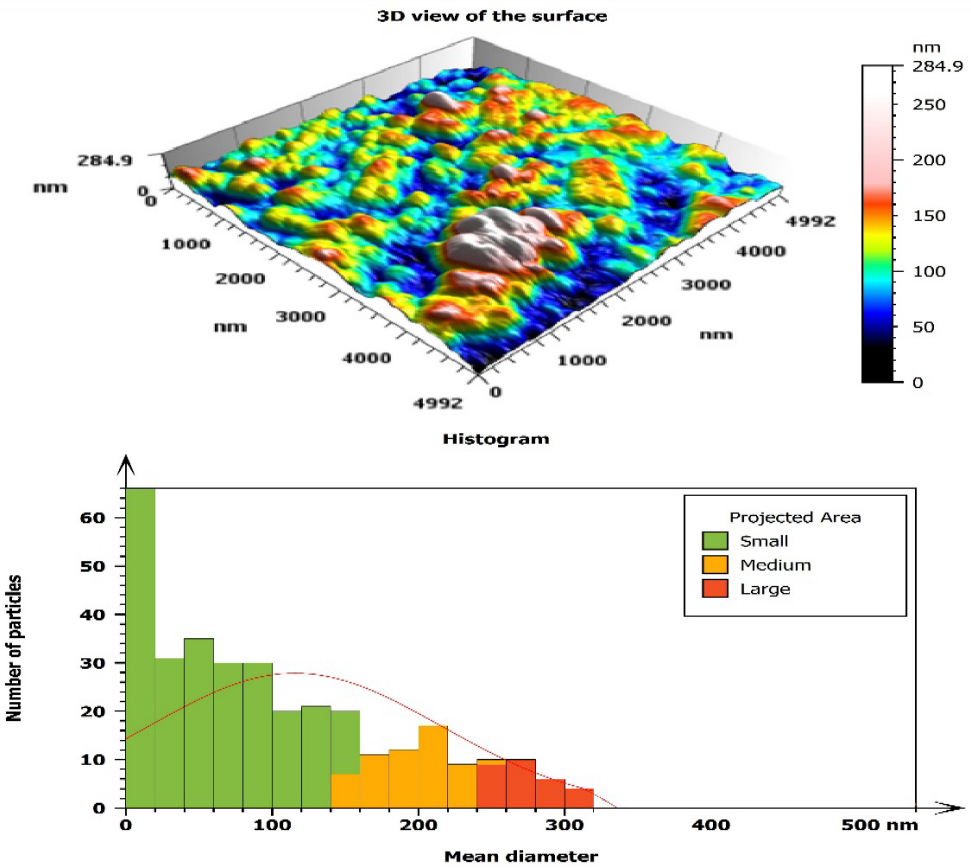

Figure 5. AFM Report and Diagram for CuNPs

efficacy in targeted cancer therapies by increasing drug delivery or causing cytotoxic effects on cancer cells. SEM pictures for CuNPs shown in Supplementary Figure 1.

Energy Dispersive X-ray (EDX)

The EDX measurement verifies the effective synthesis of copper nanoparticles (32.77 wt%), confirming the creation of metallic copper and some of copper oxides. The oxygen concentration (25.10 wt%) indicates considerable oxidation, most likely resulting in copper oxides (CuO or Cu_2O), which enhance stability and contribute to antibacterial and anticancer characteristics. Organic residues, including carbon (24.75 wt%) and nitrogen (5.64 wt%), are derived from the *Passiflora* extract utilized in the green synthesis process and act as capping agents, preventing aggregation and improving biocompatibility. Trace levels of phosphorus (7.18 wt%), Sulphur (2.33 wt%), and potassium (2.23 wt%) show the presence of phytochemicals within the plant extract, which enhances the nanoparticles' antioxidant capacity. This elemental composition demonstrates the efficiency of the green synthesis approach, which yields stable and functional copper nanoparticles appropriate for antioxidant, antibacterial, as well as anticancer applications. The results of EDX analysis for CuNPs shown in Supplementary Figure 2 and Table 2.

X-ray Diffraction (XRD)

The X-ray diffraction (XRD) pattern shown corresponds to a material analyzed with copper (Cu) as the target radiation, revealing important information about its crystalline structure and purity. The diffraction peaks at various 2θ values correspond to crystallographic planes (111), (200), (220), (311), and (222), indicating a highly crystalline material. The strength and sharpness of the peaks, notably at the (111) and (200) planes, indicate a face-centered cubic (FCC) structure, which is typically found in metallic copper or copper-based compounds. The absence of additional peaks or distortions indicates that the substance is phase-pure, with little impurities or secondary phases. Furthermore, the narrow peak widths imply a tiny crystallite size, which can be calculated using the Scherrer equation to offer more quantitative information on the material's structural features. This high level of crystallinity and structural integrity suggests that the material is suitable for use in disciplines such as electronics, catalysis, and nanotechnology. Furthermore,

Table 2. The Concentration of the Elements in the CuNPs Sample

Elements	Weight %
C	24.75
N	5.64
O	25.1
P	7.18
S	2.33
K	2.23
Cu	32.77

Table 3. Antioxidant Capacity and IC_{50} for CuNPs, Passiflora Extract, and Standard Vitamin C

CuNPs		Passiflora extract		Standard Vitamin C	
Concentration µg\ml	Inhibition %	Concentration µg\ml	Inhibition %	Concentration µg\ml	Inhibition %
25	33.12	25	19.56	25	43.12
50	42.16	50	27.9	50	50.1
100	51.41	100	35.12	100	59.86
150	61.64	150	43.61	150	71.65
200	70.35	200	51.42	200	82.31
300	81.5	300	62.81	300	91.423
IC_{50}= 98.94 µg\ml		IC_{50}= 202.25 µg\ml		IC_{50}= 46.56 µg\ml	

Table 4. Antimicrobial Activity and Inhibition Diameter for CuNPs and Passiflora Extract.

Microbial name	CuNPs	Passiflora extract
Escherichia coli	13 mm	-
Klebsiellasp	12 mm	-
Staphylococcus epidermidis	14 mm	-
Staphylococcus aureus	15 mm	-
Candida albicans	14 mm	-

the alignment of this XRD pattern with standard JCPDS data for copper or related compounds demonstrates the analysis's correctness. The presence of dominating lattice planes, particularly (111) and (200), emphasizes the material's suitability for surface-related applications such as adsorption and chemical reactivity.

Quantitative determination of Free radical scavenging activity assay (DPPH method)

After a successful synthesis for CuNPs, antioxidant capacity were done using DPPH as an oxidative stress substance. The antioxidant activity data show that copper nanoparticles, *Passiflora* extract, and normal Vitamin C all limit antioxidant activity at different doses. The nanoparticles showed a concentration-dependent inhibition, achieving 81.5% at 300 µg/ml and an IC_{50} value of 98.94 µg/ml, showing significant antioxidant capability. *Passiflora* extract inhibited 62.81% at 300 µg/ml with an IC_{50} of 202.25 µg/ml, indicating moderate action. These data demonstrate the copper nanoparticles' greater antioxidant potential compared to the plant extract. The nanoparticles' improved activity can be due to their nanoscale size, which provides a larger surface area for reactive oxygen species (ROS) neutralization. This enhances their prospective usage in antioxidant-related applications, and the green synthesis approach improves their biocompatibility as well as eco-friendliness. The results of the antioxidant capacity shown in Supplementary Figure 3 and Table 3.

Antibacterial activity for Passiflora flower leaves and CuNPs

Antimicrobial and antifungal data show that copper nanoparticles (CuNPs) significantly suppress all tested microbial strains, whereas *Passiflora* extract has no detectable antimicrobial action. CuNPs had inhibitory zones of 13 mm for *E. coli*, 12 mm for *Klebsiella* sp., 14 mm for *S. epidermidis*, and 15 mm for *Staphylococcus aureus*, demonstrating broad-spectrum efficacy versus both Gram-negative as well as Gram-positive bacteria. The strongest inhibition was reported against *S. aureus*, indicating potential application in treating antibiotic-resistant pathogens. CuNPs also demonstrated antifungal efficacy with a 14 mm inhibitory zone against *Candida albicans*, highlighting their flexibility. The lack of activity in *Passiflora* extract implies that, while it does not directly inhibit microbial growth, it is essential in the environmentally benign synthesis of CuNPs. These findings emphasize CuNPs' significant antibacterial potential for use in medical and industrial applications, including the development of antimicrobial coatings and treatments to combat resistant diseases. Antibacterial activity shown in Supplementary Figure 4, 5 and Table 4.

Table 5. Effect of CuNPs on MCF7 Breast Cancer Cell Line with Different Concentration, IC_{50} % for Inhibition Activity

Concentration (µg/ml)	Number of replication for each concentration	Growth inhibition (mean ± SE [a])
		24 hr.
0.5	4	17.1 ± 0.69
1	4	20.4 ± 2.4
10	4	21.3 ± 1.3
25	4	41 ± 1.65
50	4	51.7 ± 1.32
IC_{50}	4	47.01 µg/ml

Table 6. Effect of CuNPs on HFF Breast Cancer Cell Line with Different Concentration, IC_{50} % for Inhibition Activity

Concentration (µg/ml)	Number of replication for each concentration	Growth inhibition (mean ± SE [a]) 24 hr.
0.5	4	0 ± 0
1	4	4.04 ± 2.1
10	4	7.35 ± 0.6
25	4	14.03 ± 1.2
50	4	18.89 ± 1.5
IC_{50}	4	128.35 µg/ml

Anticancer activity for Passiflora flower leaves and CuNPs

The results show the effect of copper nanoparticles (CuNPs) on both the MCF7 breast cancer cell line along with normal HFF cells. The findings are summarized below. CuNPs treatment inhibited MCF7 cancer cell growth in a dose-dependent manner, with a maximal inhibition of 51.7 ± 1.32% at a dosage of 50 µg/ml. The IC_{50} value for the MCF7 cell line was 47.01 µg/ml, showing considerable cytotoxicity against cancer cells. HFF normal cells showed moderate growth suppression at all concentrations examined, with the maximum inhibition of 18.89 ± 1.5% at 50 µg/ml (Supplementary Figure 6). The IC_{50} for HFF cells was much higher at 128.35 µg/ml, indicating CuNPs' preferential cytotoxic effect on cancer cells over normal cells. Microscopy pictures complement these findings, revealing different morphological alterations and cell destruction in MCF7 cancer cells (Supplementary Figure 7), but HFF cells (Supplementary Figure 8) maintained structural integrity under similar treatment settings. These findings indicate that CuNPs have excellent anticancer activities and selective toxicity, underlining their potential use in cancer therapy. Tables and figures show detailed data on growth inhibition percentages and IC_{50} values (Tables 5,6).

Discussion

The study looks at the green synthesis of copper nanoparticles (CuNPs) with *Passiflora* flower extract, emphasizing the use of eco-friendly and sustainable approaches in nanoparticle production. The bioactive chemicals found in the extract were used as reducing and capping agents during the synthesis process, allowing copper salts to be converted into stable CuNPs. This green technique eliminates the requirement for toxic reducing chemicals, guaranteeing that the process is environmentally compatible, consistent with findings in other green synthesis investigations [22, 23]. The UV-Vis spectroscopy investigation confirmed the creation of CuNPs, with a characteristic plasmon resonance peak seen at 580 nm, which corresponds to the usual signatures of copper nanoparticles reported in prior research [24]. Fourier-transform infrared spectroscopy (FTIR) revealed other functional groups such as phenols, flavonoids, and terpenoids, which had a dual purpose in lowering copper ions and stabilizing the nanoparticles, Similar results were reported in investigations employing plant-derived biomolecules for nanoparticle stabilization [25]. The X-ray diffraction (XRD) investigation verified that the synthesized CuNPs were crystalline, with diffraction peaks corresponding to copper's face-centered cubic (FCC) structure. The average crystallite size, determined using the Scherer equation, was around 12 nm, which is comparable with previous results on green-synthesized copper nanoparticles [26]. Scanning electron microscopy (SEM) demonstrated a primarily spherical morphology with uniform size distribution and negligible aggregation, emphasizing the *Passiflora* extract's efficiency in maintaining nanoparticle stability [27]. The study also used the DPPH assay to assess CuNPs' antioxidant properties. CuNPs inhibited free radicals by 81.5% at 300 µg/ml and had an IC_{50} of 98.94 µg/ml. This activity far outperformed that of the *Passiflora* extract alone, demonstrating the function of nanoparticles in increasing the bioavailability and reactivity of bioactive chemicals. CuNPs' remarkable antioxidant activity is due to their high surface-to-volume ratio, which intensifies their interaction with reactive oxygen species (ROS) [28]. This mechanism has been extensively documented in the literature, notably in relation to green-synthesized metallic nanoparticles [29].

CuNPs demonstrated broad-spectrum antibacterial action against Gram-positive, Gram-negative, and fungi [30], with inhibition zones spanning from 12 to 15 mm. CuNPs' antibacterial capabilities are principally due to their ability to break microbial cell membranes and create ROS, which results in oxidative stress and cell death [31]. Prior investigations have shown that green-synthesized CuNPs had better bactericidal and fungicidal capabilities than chemically synthesized counterparts [32]. CuNPs showed considerable anticancer activity against the MCF7 breast cancer cell line, with an IC_{50} concentration of 47.01 µg/ml. This cytotoxicity was dose-dependent and accompanied by unique morphological changes, such as cell shrinkage and membrane rupture, which are signs of apoptosis [33]. CuNPs had negligible effects on HFF normal cells, with an IC_{50} of 128.35 µg/ml, indicating their selective toxicity. The preferential targeting of cancer cells is consistent with the enhanced permeability and retention (EPR) effect, which enhances nanoparticle accumulation in tumor tissues due to leaky vasculature [34]. Furthermore, the significance of copper ions in modifying redox balance within cancer cells, leading to increased oxidative stress and death, has been well documented [35]. While the findings demonstrate CuNPs' promise as multifunctional therapeutic agents, the study also identifies areas that require more exploration. The scalability of the green synthesis process for industrial applications, as well as the long-term stability and biocompatibility of CuNPs in *in vivo* systems, remain significant difficulties. Furthermore, the precise processes underlying the selective targeting of cancer cells and the synergistic effects of bioactive chemicals in *Passiflora* extract require further investigation.

Author Contribution Statement

Ons hussain works on Conceptualization, Funding acquisition, Methodology Project administration, Investigation, Validation Lubna zuhair, and Montadher Ali works on Visualization, Software, Formal analysis, Writing-original draft, Writing-review and editing, All authors have read and agreed to the published version of the manuscript.

Acknowledgements

The authors gratefully thanks national leading center of cancer research, Baghdad university for providing lab facilities and instruments . The authors are also thankful to CAC company for their role in providing some of instruments to exam the samples.

Data Availability Statement

The raw data used and/or analyzed during the current study will be available from the corresponding author on reasonable request.

Conflicts of Interest

The authors declare that there is no conflict of interest.

References

1. Singh N, Kumar B, Usman UL, Susan MABH. Nano revolution: exploring the frontiers of nanomaterials in science, technology, and society. Nano-Structures & Nano-Objects. 2024;39(8):101299. https://doi.org/10.1016/j.nanoso.2024.101299.
2. Crisan MC, Teodora M, Lucian M. Copper nanoparticles: Synthesis and characterization, physiology, toxicity and antimicrobial applications. Appl Sci. 2021;12(1):141. https://doi.org/10.3390/app12010141.
3. Babatunde DE, Denwigwe IH, Babatunde OM, Gbadamosi SL, Babalola IP, Agboola O. Environmental and societal impact of nanotechnology. IEEE Access. 2019 Dec 23;8:4640-67.
4. Ahmed SF, Mofijur M, Rafa N, Chowdhury AT, Chowdhury S, Nahrin M, et al. Green approaches in synthesising nanomaterials for environmental nanobioremediation: Technological advancements, applications, benefits and challenges. Environ Res. 2022;204(Pt A):111967. https://doi.org/10.1016/j.envres.2021.111967.
5. Mahdi MA, Mohammed MT, Jassim AN, Taay YM. Green synthesis of gold NPs by using dragon fruit: Toxicity and wound healing. InJournal of Physics: Conference Series: IOP Publishing; 2021.
6. Ożarowski M, Karpiński TM. Extracts and flavonoids of passiflora species as promising anti-inflammatory and antioxidant substances. Curr Pharm Des. 2021;27(22):2582-604. https://doi.org/10.2174/1381612826666200526150113.
7. Loganathan S, Selvam K, Govindasamy M, Habila M. Bioynthesis and characterization of zinc oxide nanoparticles (zno-nps) using passiflora foetida linn leaves extract and their biological applications. Biomass Convers Biorefin. 2024;15:5861-71. https://doi.org/10.1007/s13399-024-05593-3.
8. Abdulla KN, Abid SJ, Al-Darraji ATM. Epidemiological correlation of breast cancer with cervical cancer. World Bulletin of Public Health. 2022;11:92-5.
9. Korde LA, Somerfield MR, Carey LA, Crews JR, Denduluri N, Hwang ES, et al. Neoadjuvant chemotherapy, endocrine therapy, and targeted therapy for breast cancer: Asco guideline. J Clin Oncol. 2021;39(13):1485-505. https://doi.org/10.1200/jco.20.03399.
10. Surya C, Lakshminarayana ABV, Ramesh SH, Kunjiappan S, Theivendren P, Santhana Krishna Kumar A, et al. Advancements in breast cancer therapy: The promise of copper nanoparticles. J Trace Elem Med Biol. 2024;86:127526. https://doi.org/10.1016/j.jtemb.2024.127526.
11. Banu KS, Cathrine L. General techniques involved in phytochemical analysis. Int J Adv Res Chem Sci. 2015;2(4):25-32.
12. Sunitha M, Devaki K. Antioxidant activity of passiflora edulis sims leaves. Indian J Pharm Sci. 2009;71(3):310-1. https://doi.org/10.4103/0250-474x.56038.
13. Montadher A, Mahdi M, Mohammed M, Mohammed A, Mohammed noori jassim A, Mohammed A. Phytochemical content and anti-oxidant activity of hylocereus undatus and study of toxicity and the ability of wound treatment. Plant Archives. 2018;18:2672-80.
14. Rizwana H, Al Otibi F, Al-Malki N. Chemical composition, FTIR studies and antibacterial activity of Passiflora edulis f. edulis (Fruit). J Pure Appl Microbiol. 2019;13(4):2489-98.
15. Paulraj JA, Subharamanian H, Suriyamoorthy P, Kanakasabapathi D. Phytochemical screening, GC-MS analysis and enzyme inhibitory activity of Passiflora foetida L. Indo Am J Pharm Res. 2014;4(8):3526-34.
16. Suresh Chand M, Anita D, Chanda Kumari G, Rohini T. Green synthesis of copper nanoparticles using celastrus paniculatus willd. Leaf extract and their photocatalytic and antifungal properties. Biotechnol Rep. 2020;27:e00518. https://doi.org/10.1016/j.btre.2020.e00518.
17. Indhu A, Dharmalingam G. Oxidative and Colloidal Kinetics of Size-Controlled Copper Structures through Surface Plasmon-Regulated Examinations for Broadband Absorbance. ChemistrySelect. 2024;9(16):e202305087. https://doi.org/10.21203/rs.3.rs-3549175/v1.
18. Patel K, Solanki GK, Patel K, Pathak V. X-ray diffraction analysis of hexagonal klockmannite cuse nanoparticles for photodetectors under uv light. J Phys Chem C. 2021;125(6). https://doi.org/10.1021/acs.jpcc.0c09353.
19. Balouiri M, Sadiki M, Ibnsouda SK. Methods for in vitro evaluating antimicrobial activity: A review. J Pharm Anal. 2016;6(2):71-9. https://doi.org/10.1016/j.jpha.2015.11.005
20. Muafaq Said A, Abdulla KN, Ahmed NH, Yasin YS. Antiproliferative impact of linagliptin on the cervical cancer cell line. Asian Pac J Cancer Prev. 2024;25(9):3293-300. https://doi.org/10.31557/apjcp.2024.25.9.3293.
21. Riss TL, Moravec RA, Niles AL, Duellman S, Benink HA, Worzella TJ, Minor L. Cell viability assays. Assay guidance manual [Internet]. 2016 Jul 1.
22. Jadoun S, Arif R, Jangid N, Meena R. Green synthesis of nanoparticles using plant extracts: A review. Environ Chem Lett. 2021;19:355–74. https://doi.org/10.1007/s10311-020-01074-x.
23. Mittal AK, Chisti Y, Banerjee UC. Synthesis of metallic nanoparticles using plant extracts. Biotechnol Adv. 2013;31(2):346-56. https://doi.org/10.1016/j.biotechadv.2013.01.003.
24. Woźniak-Budych MJ, Staszak K, Staszak M. Copper and copper-based nanoparticles in medicine-perspectives and challenges. Molecules. 2023;28(18). https://doi.org/10.3390/molecules28186687.
25. Asghar MA, Asghar MA. Green synthesized and characterized copper nanoparticles using various new plants extracts aggravate microbial cell membrane damage after interaction with lipopolysaccharide. Int J Biol Macromol. 2020;160:1168-76. https://doi.org/10.1016/j.ijbiomac.2020.05.198.
26. Bin Mobarak M, Hossain MS, Chowdhury F, Ahmed S. Synthesis and characterization of cuo nanoparticles utilizing waste fish scale and exploitation of xrd peak profile analysis for approximating the structural parameters. Arab J Chem. 2022;15(10):104117. https://doi.org/10.1016/j.arabjc.2022.104117.
27. Bharathi J, S R S. Larvicidal activity of cuo and zno nanoparticles against aedes aegypti and anopheles stephensi mosquito vectors-a greener approach by phaseolus vulgaris l. Aqueous extract as bio-reductant. Results Chem. 2024;7:101408. https://doi.org/10.1016/j.rechem.2024.101408.
28. dos Santos Batista JG, Vigilato Rodrigues MÁ, de Freitas LF, Moreira Fonseca AC, de Souza Rodrigues A, Cunha da Cruz CP, et al. Copper-Based Nanomaterials for Biologically Relevant Compounds. Copper-Based Nanomaterials in Organic Transformations. 2024:305-38.

29. Shafey A. Green synthesis of metal and metal oxide nanoparticles from plant leaf extracts and their applications: A review. Green Process Synth. 2020;9:304-39. https://doi.org/10.1515/gps-2020-0031.
30. Almahdy AG, El-Sayed A, Eltarahony M. A novel functionalized cuti hybrid nanocomposites: Facile one-pot mycosynthesis, characterization, antimicrobial, antibiofilm, antifouling and wastewater disinfection performance. Microb Cell Fact. 2024;23(1):148. https://doi.org/10.1186/s12934-024-02400-6.
31. Mammari N, Lamouroux E, Boudier A, Duval RE. Current knowledge on the oxidative-stress-mediated antimicrobial properties of metal-based nanoparticles. Microorganisms. 2022;10(2). https://doi.org/10.3390/microorganisms10020437
32. Mallick S, Sabui P. Green Synthesis of Copper and Copper-Based Nanoparticles for Their Use in Medicine: Toxicity and Safety. Nanotechnology in medicine: toxicity and safety. 2021 Dec 3:174-94.
33. Luque-Jacobo CM, Cespedes-Loayza AL, Echegaray-Ugarte TS, Cruz-Loayza JL, Cruz I, de Carvalho JC, et al. Biogenic synthesis of copper nanoparticles: A systematic review of their features and main applications. Molecules. 2023;28(12). https://doi.org/10.3390/molecules28124838
34. Maeda H, Nakamura H, Fang J. The epr effect for macromolecular drug delivery to solid tumors: Improvement of tumor uptake, lowering of systemic toxicity, and distinct tumor imaging in vivo. Adv Drug Deliv Rev. 2013;65(1):71-9. https://doi.org/10.1016/j.addr.2012.10.002.
35. Liu J, Yuan Y, Cheng Y, Fu D, Chen Z, Wang Y, et al. Copper-based metal-organic framework overcomes cancer chemoresistance through systemically disrupting dynamically balanced cellular redox homeostasis. J Am Chem Soc. 2022;144(11):4799-809. https://doi.org/10.1021/jacs.1c11856.